

FLEXURAL BEHAVIOR OF HIGH STRENGTH FIBER REINFORCED CONCRETE BEAMS AS AFFECTED BY RIB GEOMETRY AND GRADE OF MAIN STEEL UNDER STATIC LOADS

Rashwan M. M. ; Hosny M. Soghair ; Aly Abdel-Zaher ELSayed

Civil Engineering Department, Faculty of Engineering, Assiut University, Assiut, Egypt

Ali Mohamed Abdallah Abou-Zied (Ph. D. Student)

General Authority of Educational Buildings, Sohag, Egypt

(Received February 19, 2006 Accepted April 8, 2006)

The need of high-performance concrete is increasing in recent years for the use in high rise building and the new breed of concrete gravity platforms for offshore structures. The use of high strength concrete needs high percentage of steel reinforcement to get the full capacity of the flexural strength of the member. Hence, the need of using high grade of steel reinforcement and different fibers to concrete mixes is necessary from the economical point of view. So, different ribs are used for the increase of bond strength between steel reinforcement and high-performance concrete. But these materials were brittle and the failure also was brittle. So, fibers are used to enhance their composite properties.

There is little information in the available literature about the flexural behavior of high-performance and high-performance fiber-reinforced concrete beams with different rib geometry under partial bond. Therefore, this paper focuses on the application of different types of fibers and steel rib geometry in the technology of high strength R.C. rectangular beams having $f_c=900\text{kg/cm}^2$ and study their flexural behavior under static loading.

Test results showed that, the failure mode, cracks pattern and flexural behavior of high strength and fiber-high strength reinforced concrete beams were clearly affected by rib geometry and quality of the main steel and fibers type. The values of cracking and ultimate load carrying capacity of R.C. tested beams were increased with the increase of the grade of the main steel and its relative rib area (F_y from 3100 to 4750 kg/cm^2 & α_{sb} from 0.0 to 0.10) by about 65 & 76% respectively for beams without fibers. Also, they were increased by about 80 & 82% for beams with polypropylene fibers and by about 86 & 83% for beams with harex steel fibers. The addition of fibers to concrete mixes of R.C. beams has greatly improved their ductility by increasing the ultimate strains under maximum compressive stresses and improved the crack propagation patterns for all tested (HPFRC) beams.

KEYWORDS: Rib geometry, Fibers, polypropylene, harex steel fibers, Flexural behavior, High-performance concrete, cracks pattern, failure mode

1-INTRODUCTION

High strength concrete began to be developed in 1970 for the use in high rise buildings and the new breed of concrete gravity platforms for offshore structure. These developments have continued over the past twenty-years with concrete of 80,100 and 120 N/mm² and even higher. According to ACI building code [1], the maximum allowable percentage of reinforcement varies from 1% to 4.7% for normal strength concrete having $f_c=300\text{kg/cm}^2$ and steel with $f_y=2400\text{kg/cm}^2$. But, this percentage varies from 1% to 7% for high performance concrete having $f_c>800\text{kg/cm}^2$ and steel with $f_y=4000\text{kg/cm}^2$. So, the use of high strength concrete needs high percentage of steel reinforcement to get the full capacity of the flexural strength of the member. So, the need of using high grade of steel reinforcement and different fibers to concrete mixes is necessary from the economical point of view. Using steels of high grade maximizes the benefit of using this material. So, different ribs are used for the increase of bond strength between steel reinforcement and high-performance concrete. But these materials were brittle and their failure also was brittle. So, fibers are used to enhance composite properties. The enhanced properties include tensile strength, compressive strength, bond strength, elastic modulus, crack resistance, crack control, durability, fatigue life, resistance to impact and abrasion, shrinkage, expansion, thermal characteristics, and fire resistance [2, 3, 4].

High-performance Fiber-Reinforced Concrete (HPFRC) is a result of the addition of either short discrete fibers or continuous long fibers to the cement based matrix. Due to the superior performance characteristics of this category of (HPC), its use by the construction industry has significantly increased in the last 16 years. A very good guide to various Portland cement-based composites as well as their constituent materials is available in a published book "Balaguru and Shah 1992" [5]. The book provides information on fabrication, mechanical and long-term properties of concrete with short discrete fibers. It also covers special topics such as fiber-reinforced cements and slurry-infiltrated fiber concrete. In 1992, the first international workshop on high performance fiber reinforced cement composites (HPFRCC) was held in Mainz, Germany "Reinhardt and Naaman 1992" [6].

M. H. Harajli and M. E. Mabsout, 2002, [7] have studied the effect of fibers on the bond strength of deformed bars embedded in concrete. They have reported that, the use of fiber reinforcement significantly increases the development/splice strength and considerably enhances the ductility of bond failure. The increase in bond strength required using steel fibers may increase with levels substantially larger than the maximum limit stipulated in the ACI building code [1] for ordinary transverse reinforcement.

Experimental study on steel fiber-reinforced concrete beams were investigated by Magdy A. Tayel et al, 2003, [8]. They concluded that the addition of steel fibers to a concrete mix has increased the hardened concrete compressive and tensile strengths. And the addition of steel fibers in a very small ratio = 0.25% does not increase the concrete strengths.

The effect of rib geometry of steel reinforcement on bond of normal strength concrete was studied by Ali M.A., 2000, [9]. He found that the final mode of failure, cracking and ultimate load and deformation of cantilever-to-column connection were affected

by the relative rib area (α_{sb}) and development length . The geometry of the ribs can be expressed by the relative rib area α_{sb} , which is described by Rehm [10] as α_{sb} (ratio of projected rib area normal to bar axis to the product of the nominal bar perimeter and the center-to-center rib spacing). Rehm[10], Soretz and Holzenbein[11], and Parviz [12] showed that the influence of the deformation pattern of bar on the local bond stress-slip behavior can reasonably be described as a function of the relative rib area for pullout specimens with normal concrete strength.The definition of the relative rib area α_{sb} is described by Rehm as shown in **Fig. 1**.

$$\alpha_{sb} = (k \cdot F_R \cdot \sin\beta) / (\pi \cdot db \cdot c_s) \dots \dots \dots (1)$$

Where :

k = number of transverse ribs around the bar perimeter

db = nominal diameter of bar , and F_R = parabolic area of the transverse rib.

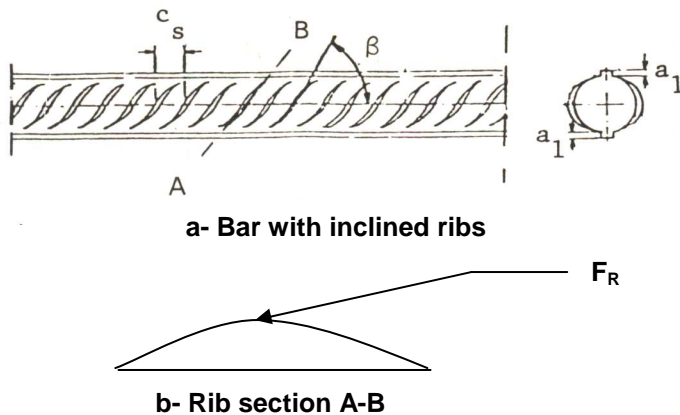


Fig. 1: Properties of the rib geometry of steel bar.

Since 1990, several studies have been conducted to investigate specifically the bond strength of reinforcement in high strength concrete. de Larrard et al. , 1993, [13] evaluated the bond strength between high strength concrete and reinforcing bars using the RILEM beam test. A high strength concrete with 28-days compressive strength of 95 MPa was used and a normal strength concrete of 42 MPa used as a control. Three different sizes of deformed bars (10, 16, 25 mm) and one smooth bar (25 mm) were used. Based on several preliminary tests, the RILEM recommended bond (anchorage) length of 10 times bar diameter had to be reduced to 3 times to 2.5 times bar diameter for high strength concrete to ensure bond failure rather than yielding of reinforcement. So, this paper focuses on the application of different types of fibers and different grades of steel with different shapes of rib geometry in the technology of high strength R.C. rectangular beams having $f_c = 900\text{kg/cm}^2$ under static loading.

2- EXPERIMENTAL PROGRAM

The main aim of this program is to investigate experimentally the behavior of high strength R.C. rectangular beams affected by fibers and grade of main steel with different types of rib geometry under static loads.

The experimental approach in this study consisted of testing nine rectangular beams under static load. High strength concrete of about 900kg/cm^2 compressive strength was used. All beams were tested at 28 days curing age. The beams were all identical in size, 12-cm width and 30 cm overall depth. Bonded parts beyond the support (L_1) for steel reinforcement used in this study were $5d_b$ only for all beams. All beams were tested under two third points of loading on an effective span of 2.4ms, with shear span to effective depth ratio $a/d = 3.0$. The steel reinforcement of all beams was $2\phi 16\text{mm}$ as tension reinforcement, $2\phi 12\text{mm}$ as compression reinforcement and closed stirrups of $10\phi 8\text{mm}$. Details of tested beams and reinforcement are shown in **Fig. 2**. The study takes into consideration the following variables:

- 1- Grade of the main steel represented by its yield stress ($F_y = 3100, 4600 \text{ \& } 4750 \text{ kg/cm}^2$),
- 2- Rib geometry of the main steel reinforcement used in the tested beams, which represented by its relative rib area ($\alpha_{sb} = 0.00, 0.062 \text{ \& } 0.10$).
- 3- Type of fibers: two types of fibers (polypropylene, and steel fibers "harex") were used for all high strength fiber reinforced concrete beams.

The behavior of tested beams includes the initiation of cracks and their propagation, final mode of failure, relationship between applied flexural load and maximum induced deformation; in terms of deflection, slip, strain and end slope of (HPC) and (HPFRC) beams reinforced with steel having variable relative rib area (α_{sb}) and modified with different types of fibers.

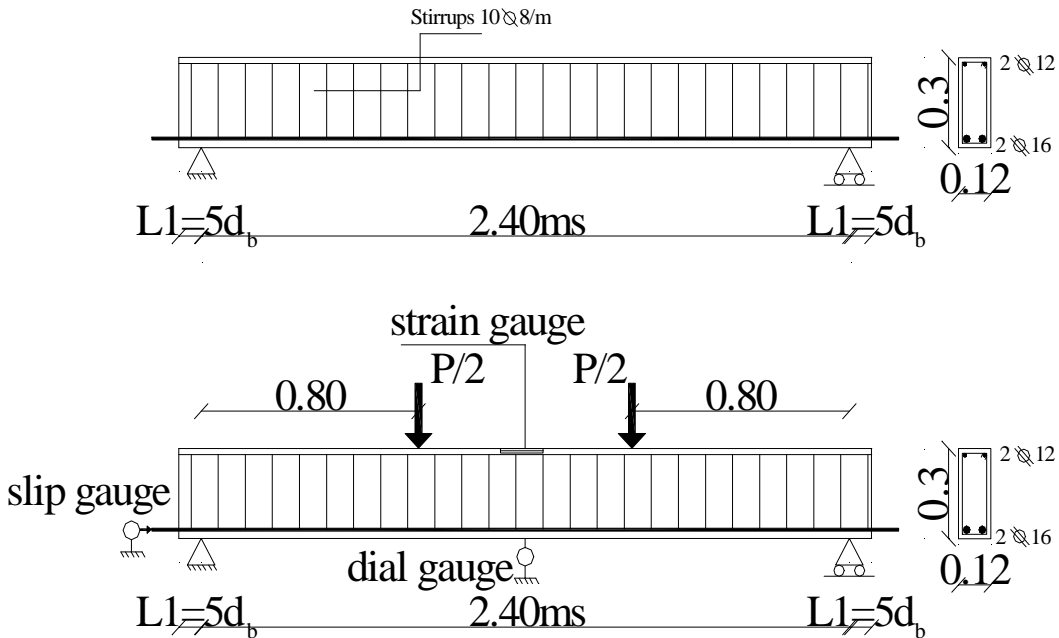


Fig. 2: Details of R.C. tested beams.

2.1- Materials

2.1.1- High Performance Concrete (HPC)

Concrete mix design was made to produce high strength concrete of 28-days cubic strength of 900 kg/cm². Concrete mix proportions are given in **Table 1**.

Table 1: Concrete mix proportions.

Cement, kg/m ³	Fine aggregate, kg/m ³	Coarse aggregate, kg/m ³	Silica-fume, kg/m ³	Superplasticizer (B.V.S.), Litre/m ³	Water, liter/m ³
500	580	1200	110	17.5	140

Ordinary Portland cement was used (Assiut Cement). The coarse aggregate used was crushed basalt of 12mm nominal size. Local natural sand was used as fine aggregate; Superplasticizer (B.V.S.) type, with optimum dosage 17.5 litre/m³ for concrete mix; 110 kg/m³ optimum dosage of silica fume with specific gravity 2.15 t/m³ were used.

2.1.2- Steel Reinforcement

Plain bars of normal mild steel ($F_y = 3100$ kg/cm² with $\alpha_{sb} = 0.00$) with diameters 8 and 16-mm used for stirrups and main steel in (HPC) and (HPFRC) beams. But deformed bars of high tensile strength ($F_y = 4600$ & 4750 kg/cm² with $\alpha_{sb} = 0.062$ & 0.10, respectively) were used as longitudinal tension /compression reinforcements with diameters of 16 and 12mm in (HPFRC) beams. Details of steel reinforcement are given in **Table 2**.

2.1.3 - High-Performance Fiber-Reinforced Concrete Properties (HPFRC)

Six beams (group B&C) of high performance fiber reinforced concrete of 900 kg/cm² were made from the same materials of (HPC) plus polypropylene (B1P, B2P, and B3P) and harex steel fibers (B1S, B2S, B3S). Typical properties of various types of the non-metallic fiber (polypropylene fiber) and metallic fiber (harex steel fiber) are given in **Table 3** and the shape of fibers is shown in **Fig. 3**. One fiber concentration only was used in the all tested beams and equals to 1.0% by volume of the total mix. This concentration of polypropylene is large but it was taken in this research for the comparison of results with the harex steel fibers.

Table 2: Mechanical and Geometrical Properties of Steel Bars.

Group	Series	Nominal d_b , mm	Bar Notation	Relative Rib Area (α_{sb})	Yield stress (F_y) kg/cm ²	Ultimate strength (F_u) kg/cm ²	% Elongation
A & B and C	B1, B2, B3 & B1P, B2P, B3P and B1S, B2S, B3S	16	Sm	0.000	3100	4600	28.6
			B\S	0.062	4600	6700	19.2
			EZ•AL2	0.100	4750	6900	18.5
Top steel		12	EZAL	0.060	4600	6700	22.0
Stirrups		8	Sm*	0.000	2900	4200	29.5

Table 3 : Typical properties of fibers .

Type of fibers	Diameter, (μm)	Length, (mm)	Density, (gm/cm^3)	Tensile Strength, (kg/cm^2)	Young's modulus, (kg/cm^2)	Elongation, (%)
Polypropylene	2-20	18	0.91	5000	50000	8-10
Harex steel	1000	32	7.8	20000	2000000	3

Properties of harex steel fiber locally produced by chemicals for modern building CEM Co. But polypropylene fiber produced by Sika Co. in Italy



a-Polypropylene fiber

b-Harex steel fiber

Fig. 3: Shape of metallic and non-metallic fibers.

2.2 Test Procedure

Nine R.C. beams of 28 days age were tested, simply supported over a clear span of 2.4ms, under two third-points of loading. The available testing machine (EMS 60 tons Pu) was used in testing the beams specimens under static loading. Average values of 28-days concrete compressive strength determined from cubes of 15cm side length were (907, 900 and 918 kg/cm^2) for (HPC) beams without fibers, (HPFRC) beams with polypropylene fibers and harex steel fibers respectively. The beams deflection was measured using dial gauges with accuracy of 0.01mm at the bottom surface of testing beams at mid span. Strains of concrete were measured at the top surface of tested beams at the mid span using electrical strain gauges having effective length of 50 mm. The load was applied in an increment of 0.5 ton up to failure load. After each increment, reading of strain gauges, dial gauge, and crack propagation were recorded.

3- TEST RESULTS

3.1- Effect Of The Shape Of Rib Geometry On The Properties Of Steel Bars And Their Ultimate Bond Strength

The effect of different shapes of rib geometry, represented by relative rib area (α_{sb}), on the mechanical properties of different types of steel bars of nominal diameter 16mm and their ultimate bond strength for different bonded lengths was

studied. Also, the influence of different shapes of rib geometry, represented by relative rib area on the ultimate bond strength of different types of steel bars of the same nominal diameter was studied by using pull-out prismatic specimens of square section 12x12cms with cubic strength 900kg/cm², which were tested with 16mm embedded steel bar of different bonded lengths of 5d_b, 7.5d_b & 10d_b and the results are shown in **Table 4**. From **Table 4**, it is clear that the shape of rib geometry of steel bars represented by its relative rib area (α_{sb}) has a very small effect on their mechanical properties especially yield stress and ultimate strength. But, this shape of rib geometry has a clear influence on the ultimate bond strength of tested specimens, which increased by the increase of the relative rib area and not mainly depended on the yield stress only of steel bars. For example, by the comparison of bar type EZ.AL1 ($F_y = 4750 \text{ kg/cm}^2$ & $\alpha_{sb} = 0.07$) with bar type BS5 ($F_y = 4300 \text{ kg/cm}^2$ & $\alpha_{sb} = 0.093$) it is clear that, the ultimate bond strength of specimen with bar BS5, of low yield stress, equals 224.9 kg/cm². But, it equals 208.39 kg/cm² for specimen with bar EZ.AL1 of high yield stress. This means that the main influence on the ultimate bond strength depends on the rib geometry of the bars, which did not reach the yield point.

Table 4: Mechanical and geometrical properties of deformed Bars and their effect on the ultimate bond strength of high strength concrete prismatic specimens.

Nominal d _b , mm	Type of bars	Relative Rib Area (α_{sb})	Yield stress kg/cm ² (F _y)	Ultimate strength kg/cm ² (F _u)	% Elongation	ultimate bond strength (F _{bu}), kg/cm ² for different bonded lengths		
						5db	7.5 db	10 db
16	Sm	0.000	3100	4600	28.6	96.61	92.92	88.16
	Lxx	0.030	4600	6940	22.4	179.5	171.42	159.4
	BS	0.045	4360	6880	19.9	190.0	181.62	168.23
	EZ	0.060	4700	6990	20.3	200.8	192.15	192.15
	B\S	0.062	4600	6700	19.2	201.92	192.56	192.56
	EZ1AL	0.065	4500	6675	19.7	204.81	193.72	193.72
	EZ-AL	0.069	4600	6650	19.3	206.9	194.71	194.71
	EZ.AL1	0.070	4750	6700	18.6	208.39	195.29	195.29
	ARSL	0.072	4600	6750	18.4	210.5	196.2	196.2
	NS	0.073	4400	6450	18.6	211.3	196.54	196.54
	TS	0.076	4450	6550	19.0	212.6	196.87	196.87
	DK2	0.078	4550	6800	19.5	215.0	197.8	197.8
	DK1	0.090	4450	6200	20.5	222.0	203.1	203.1
	BS5	0.093	4300	6190	18.8	224.9	204.91	204.91
EZ.AL2	0.100	4750	6900	18.5	231.35	209.39	209.39	

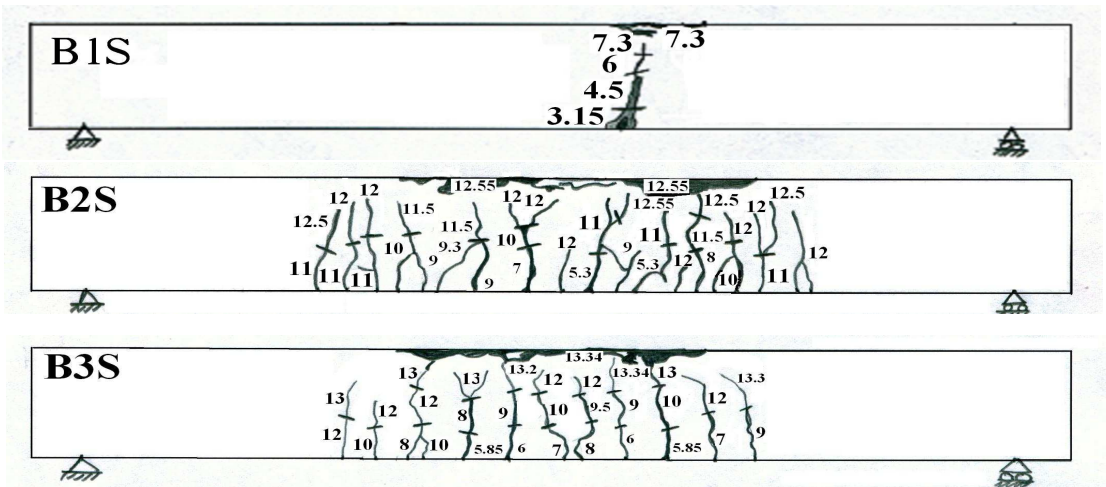


Fig. 4c: Cracks pattern of R.C. beams with harex steel fibers (B1S, B2S and B3S).



Fig. 5a: Failure shape of beam (B1).



Fig.5b: Failure shape of beam (B2).



Fig.5c: Failure shape of beam (B3).

- The major cracks were formed in the tension zone at the maximum moment for all beams (at mid span of beams).
- The final modes of failure of beams (B1, B1P, B1S) with smooth bars were noticed to be bond-flexural failure, and for ribbed bars with relative rib area (α_{sb}) = 0.062 & 0.10 as for beams (B2, B2P, B2S, B3, B3P & B3S) were noticed to be flexural failure.

3.2.2 Effect of fiber type

The following noted cracks for beams were observed as follows:

- The initiation of cracks were observed for beams without fibers (B1, B2, B3) and for beams with polypropylene fibers (B1P, B2P, B3P) or harex steel fibers (B1S, B2S, B3S) at the maximum moment in the tension zone.
- The propagation of cracks for beams (B1S, B2S, B3S) were less than those compared to beams (B1P, B2P, B3P), which were less than those compared to beams (B1, B2, B3).
- The major cracks were formed at the maximum moment for all tested beams (at mid span).
- The final modes of failure for beams (B1, B1P, B1S) with smooth bars were noticed to be bond-flexural failure, and for ribbed bars with relative rib area (α_{sb}) = 0.062 & 0.10 as for beams (B2, B2P, B2S, B3, B3P & B3S) were noticed to be flexural failure as shown in **Figs. 4, 5 and 6**.



Fig. 6a: Failure shape of beam (B1P).

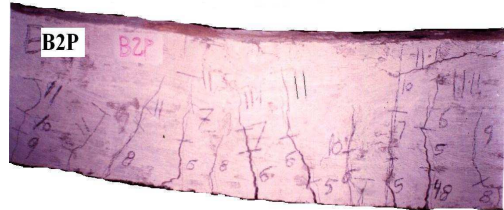


Fig. 6b: Failure shape of beam (B2P).

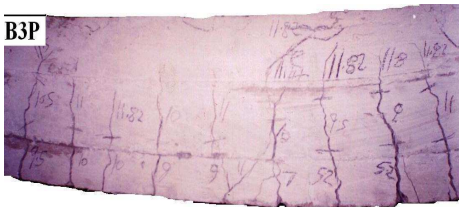


Fig. 6c: Failure shape of beam (B3P).

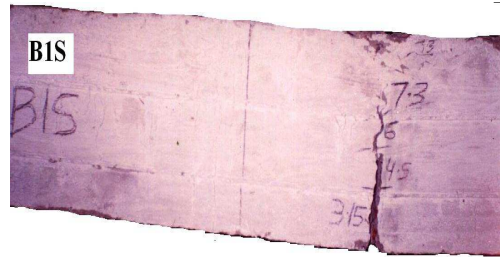


Fig. 6d: Failure shape of beam (B1S).



Fig. 6e: Failure shape of beam (B2S).



Fig. 6f: Failure shape of beam (B3S).

3-3 Measured Deformations

The flexural load-mid span deflection; load-end slip; load-concrete strain and load-end slope curves obtained from tests are shown in **Figs. 7 to 9**. The effect of the various parameters on the load-mid span deformation characteristics will be discussed as follows.

3.3.1 Load – mid span deflection

The measured and theoretical values of mid span deflection of tested beams are plotted versus applied load up to failure as shown in **Fig. 7**. All plotted values indicated that, the deflection increases as the applied load increases up to the ultimate load for all beams. Then, the beams started to show the sign of failure and the slope of the load-deflection curve becomes flat or horizontal straight line and the deflection increased with or without decrease of loads for beams with fibers. The relation between the applied load and the mid span deflection tends to be in linear or non linear relation depending on the applied load level. The relation depends mainly on the grade of the main steel and its relative rib area (α_{sb}), as well as the fiber type. The theoretical central deflection at all loads was calculated only for (HSC) beams without fiber by using ACI [1] equations as:

$$\delta_{th} = (23/648) * [(P_u/2) * L^3 / (E_c * I_e)] \dots\dots\dots (2)$$

$$E_c = 3320 \sqrt{f'_c} + 6900 \text{ Mpa} \dots\dots\dots (3)$$

$$I_e = (M_{cr}/M_a)^3 I_g + (1 - (M_{cr}/M_a)^3) I_{cr} \dots\dots\dots (4)$$

$$M_{cr} = (f_{ctr} \cdot I_g) / y_{ct}, \quad f_{ctr} = 0.94 \sqrt{f'_c} \text{ Mpa}, \quad I_g = bt^3/12, \quad y_{ct} = t/2, \quad b = 12\text{cm}, \quad t = 30\text{cm}$$

– Effect of grade of the main steel and its relative rib area (α_{sb})

The values of the applied load for all tested beams increased with the increase of grade of steel reinforcement and its relative rib area (α_{sb}). Generally, the shape of the load-mid span deflection curve of tested beams reinforced with bars of low grade and small relative rib area (α_{sb}) differs than that of tested beams with high grade of steel and high relative rib area (α_{sb}). At the same value of deflection of 1.0 mm for beams (B1, B2 & B3), the applied load increased respectively from 5.5 ton to 9.0 & 10.5 tons. This means that the increase of grade of steel from $f_y = 3100$ to 4750 kg/cm^2 and its relative rib area from 0.0 to 0.10 increased the applied load at the same deflection by about 90%.

– Effect of fibers type

The values of the applied load at all values of deflections for beams modified with polypropylene fibers were more than that values of beams without fibers. And the values of the applied load at all values of deflections for beams modified with harex steel fibers were more than that values of beams with polypropylene fibers. For high performance concrete, the failure of beams without fibers was more brittle. But For high performance fiber reinforced concrete, the failure of beams was ductile, as shown in **Fig. 7**. At the same value of deflection of 1.0 mm for beams with harex steel fibers (B1S, B2S & B3S), the applied load increased respectively from 6.8 ton to 11.5 & 13.2 tons. This means that the increase of grade of steel from $F_y = 3100$ to 4750 kg/cm^2 and its relative rib area from 0.0 to 0.10 increased the applied load at the

same deflection by about 94%. This type of fiber increased applied load at the same deflection by about 26% for beams with ribbed bars and by about 23% for beams with smooth bars.

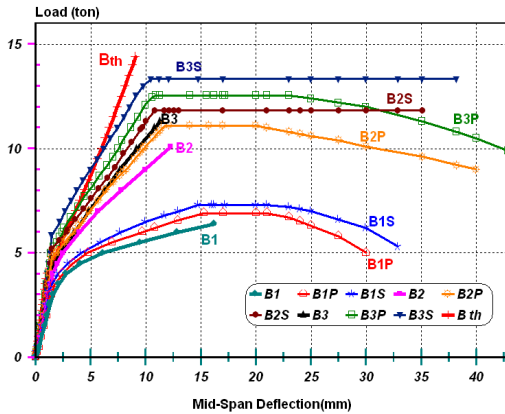


Fig. 7: Load versus mid span deflection for tested beams with and without fibers.

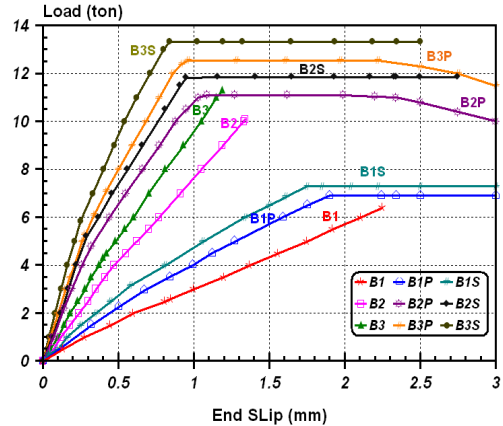


Fig. 8: Load - end slip relationship for tested beams with and without fibers.

3. 3. 2 Load – end slip relationship

Stresses for concrete and steel are transferred between the two materials if they work together in beams. The term “bond” is used to describe the means by which slip between concrete and steel is prevented or minimized wherever the tensile or compressive stress in a bar changes or not. Bond stresses must act along the surface of the bar to produce the change. Deformed bars have larger bond capacity because of the interlocking of the ribs with the surrounding concrete. The mechanism of bond is comprised of three main components: chemical adhesion, friction, and mechanical interlock between bar ribs and concrete measured. The measured slip of main steel for all tested beams is plotted against applied load up to failure as shown in **Fig. 8**.

– Effect of grade of main steel and its relative rib area (α_{sb})

The measured values of the slip for all tested beams indicated that, the end slips decrease with the increase of the grade of steel and its relative rib area (α_{sb}). Also, the load carrying capacity increases with the increase of the grade of steel and its relative rib area (α_{sb}). At the same value of slip of 1.0 mm for beams (B1, B2 & B3), the applied load increased respectively from 3 ton to 7.75 & 9.5 tons. This means that the increase of grade of steel from $f_y = 3100$ to 4750 kg/cm^2 and its relative rib area from 0.0 to 0.10 increased the applied load at the same slip by about 217 %.

– Effect of fibers type

The measured loads for tested beams group (C) having harex steel fibers were larger than that measured for group (B) having polypropylene fibers. Also, the measured loads for group (B) having polypropylene fibers were larger than that measured for group (A) without fibers as shown in **Fig. 8**. The measured end slip of steel bars

decreased for beams with fibers. At the same value of slip of 1.0 mm for beams with harem steel fibers (B1S, B2S & B3S), the applied load increased respectively from 4.75 ton to 11.8 & 13.4 tons. This means that the increase of grade of steel from $F_y = 3100$ to 4750 kg/cm^2 and its relative rib area from 0.0 to 0.10 increased the applied load at the same slip by about 182 %. This type of fiber increased applied load at the same slip by about 41 % for beams with ribbed bars and by about 57 % for beams with smooth bars.

3.3.3 Concrete strain

The measured values of concrete strain at the top surface of the compression zone of tested beams are plotted versus applied load from starting loading up to failure as shown in **Fig. 9**. Generally, the compressive concrete strain increases as the applied load increases up to the ultimate loads. The rate of increase of compressive concrete strain depends on the grade of steel reinforcement and its relative rib area (α_{sb}) and the fibers type. The effect of these parameters can be observed from such curves.

– Effect of grade of the main steel and its relative rib area (α_{sb})

The measured values of the concrete strain for all tested beams in group (A), (B) and (C) decrease with the increase of the grade of steel reinforcement and its relative rib area (α_{sb}). At the same value of concrete strain of 2×10^{-3} for beams (B1, B2 & B3), the applied load increased respectively from 6.5 ton to 10 & 11 tons. This means that the increase of grade of steel from $f_y = 3100$ to 4750 kg/cm^2 and its relative rib area from 0.0 to 0.10 increased the applied at the same strain by about 69 %.

– Effect of fibers type

The measured values of compressive concrete strain for all tested beams of group (A) increase than that of beams with the use of fibers (group B & C) as shown in **Fig. 9**. At the same value of concrete strain of 2×10^{-3} for beams with harem steel fibers (B1S, B2S & B3S), the applied load increased respectively from 7 ton to 11.9 & 13.2 tons. This means that the increase of grade of steel from $F_y = 3100$ to 4750 kg/cm^2 and its relative rib area from 0.0 to 0.10 increased the applied at the same strain by about 88 %. This type of fiber increased applied load at the same concrete strain by about 20% for beams with ribbed bars and by about 8 % for beams with smooth bars.

3.3.4 Load-slope characteristics

The maximum measured slope at the center of hinged support of the beams is plotted versus the applied load from zero loading up to failure as shown in **Fig. 10**. Generally, the slope at the center of hinged support increases as the applied load increases up to limit of cracking load. Beyond this limit a sharp decrease in the rate of increase of the ultimate slope was observed and after that increasing in the slope was accompanied by a slight increasing of the applied load up to ultimate load for all beams. Then starting from the ultimate load, the beams started to show the sign of failure and the slope of the load- slope curve becomes flat from top to bottom or horizontal straight line and the slope increased with or without decrease of the loads for beams with fibers. The effect of the studied variables on the load-end slope will be discussed as follows:

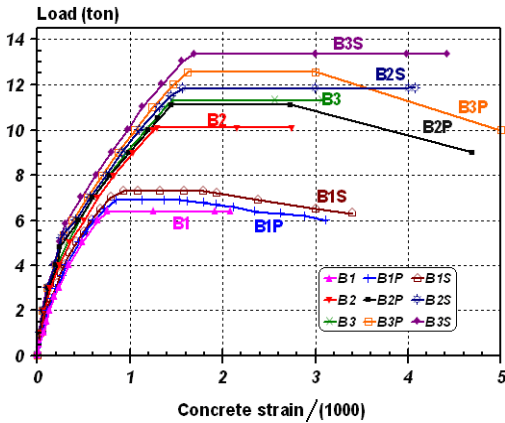


Fig. 9: Load–Compressive concrete strain at mid span relationship for tested beams.

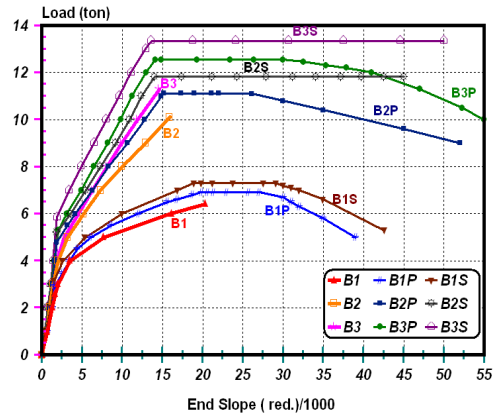


Fig. 10: Load- end slope relationship for all R.C. tested beams.

– Effect of grad of the main steel and its relative rib area (α_{sb})

The values of slope for all tested beams in groups (A), (B) and (C) decrease with the increase of the value of grade of steel and its relative rib area (α_{sb}) due to the increase of the yield stress of steel reinforcement and bond between the steel and concrete. At the same value of slope of 1.5×10^{-3} for beams (B1, B2 & B3), the applied load increased respectively from 5.8 ton to 9.8 & 11.4 tons. This means that the increase of grade of steel from $f_y = 3100$ to 4750 kg/cm^2 and its relative rib area from 0.0 to 0.10 increased the applied at the same slope by about 96 %.

– Effect of fibers type

The values of end slope for all tested beams in groups (B & C) with the used fibers were less than for beams in group (A) as a result of increasing quality of concrete and bond stresses between main steel and concrete. At the same value of slope of 1.5×10^{-3} for beams with harem steel fibers (B1S, B2S & B3S), the applied load increased respectively from 6.7 ton to 11.8 & 13.3 tons. This means that the increase of grade of steel from $F_y = 3100$ to 4750 kg/cm^2 and its relative rib area from 0.0 to 0.10 increased the applied at the same slope by about 98 %. This type of fiber increased applied load at the same slope by about 17 % for beams with ribbed bars and by about 16 % for beams with smooth bars.

4. DISCUSSIONS OF RESULTS

This item describes and interprets the analysis of the obtained test results of the HPC and HPFRC beams. The analysis includes the relationship between the values of the cracking and ultimate loads, slips, deflections, concrete strains and slope versus grade of steel represented by its yield stress or its relative rib area of bars (α_{sb}) and the used fibers type.

4.1 Cracking and Ultimate Loads

The values of the obtained cracking (P_{cr}) and ultimate loads (P_u) for tested beams are given in **Table 5**. The theoretical values of the ultimate load ($P_{u_{th}}$) can be determined

according to the smallest value of the following cases (a)- due to bending ,(b)- due to shear or(c)-due to bond .The critical case was due to bending as follow by “ACI code 1995” [1]:

$$\mu = A_s \cdot f_y \cdot d (1 - 0.59 \rho f_y / f'_c), f'_c = 0.9 f_c, P_{u_{th}} = 2.5 \mu, \mu = 0.8 (P_{u_{th}} / 2), \rho = A_s / A_c$$

$$\text{Then, } P_{u_{th}} = 2.7 F_y (1 - 0.9 F_y / 105) \text{ kg} \dots \dots \dots (5)$$

The theoretical values of the ultimate load for beams (without fibers) were 8.14 ; 11.91 and 12.28 ton for bars type Sm ; B\S and EZ•AL2, respectively .

The theoretical values of the cracking load (P_{cr}) for beams without fibers can be determined according to (ACI) [1]. Where M_{cr} = (f_{ct} .I_g)/y_{ct} , f_{ct} =0.94√f/c Mpa , M_{cr} = 0.8(P_{cr}.h/2), So, P_{cr} = 2.5M_{cr}. Then P_{cr} = 3.81 ton.

– Influence of grade of steel and its relative rib area (α_{sb})

The values of cracking (P_{cr}) and the ultimate loads (P_u) for tested beams increase with the increase of grade of steel bars represented by its yield stress and relative rib area (α_{sb}) as shown in **Table 5** and **Fig. 11**.

The values of cracking and the ultimate loads of bars (B\S) and (EZ.AL2) compared to the corresponding values of steel bar (Sm) at different fibers were increased, respectively as follows:

(a)-For cracking load

- For beams without fibers, by about 53.9 and 65.4 % , respectively.
- For beams with polypropylene fibers, by about 63.2 and 80.3 % , respectively.
- For beams with Harex steel fibers, by about 65 and 85.7% , respectively.

(b)-For ultimate load

- For beams without fibers, by about 57.8 and 76.6 % , respectively.
- For beams with polypropylene fibers, by about 61 and 81.9 % , respectively.
- For beams with H. steel fibers, by about 62 and 82.7 % , respectively.

Table 5: Values of cracking and ultimate loads for beams with and without fibers.

Group No.	Series of beams	Relative Rib Area (α _{sb})	Fiber Types	P _{cr} . (ton)	P _u . (ton)	Mode of Failure
A	B1	0.00	Without fibers	2.6	6.40	Bond -Flexural Failure
	B2	0.062		4.0	10.10	Flexural Failure
	B3	0.100		4.3	11.30	Flexural Failure
B	B1P	0.00	PP.F	2.94	6.9	Bond -Flexural Failure
	B2P	0.062	PP.F	4.8	11.11	Flexural Failure
	B3P	0.100	PP.F	5.3	12.55	Flexural Failure
C	B1S	0.00	HS.F	3.15	7.3	Bond -Flexural Failure
	B2S	0.062	HS.F	5.2	11.82	Flexural Failure
	B3S	0.100	HS.F	5.85	13.34	Flexural Failure

P_{cr} and P_u : Experimental values of cracking and ultimate load

- Influence of fibers type

The values of cracking (P_{cr}) and ultimate loads (P_u) for tested beams were more for beams with harex steel fibers than those of beams with polypropylene fibers. Also, they were more for beams with polypropylene fibers than those of beams without fibers as shown in **Fig. 12**. The values of cracking (P_{cr}) and ultimate (P_u) loads of beams made from (HPFRC) with harex steel and polypropylene fibers compared to the corresponding values of beams made from (HPC) without fibers with steel bars type (Sm), (B\S) and (EZ.AL2) were increased respectively as follows:

(a) For cracking load

For bar (Sm), by about 13.07 and 21.15%, respectively.

For bar (B\S), by about 20.0 and 30.0 %, respectively

For bar (EZ.AL2), by about 23.2 and 36.04%, respectively.

(b) For ultimate load

For bar (Sm), by about 7.8 and 14.08 %, respectively

For bar (B\S), by about 10 and 17.03 %, respectively.

For bar (EZ.AL2), by about 11.06 and 18.05 %, respectively.

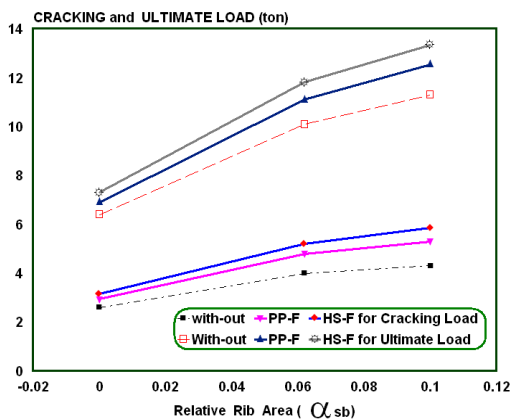


Fig (11): Cracking and ultimate loads of tested beams versus relative rib area of steel bars.

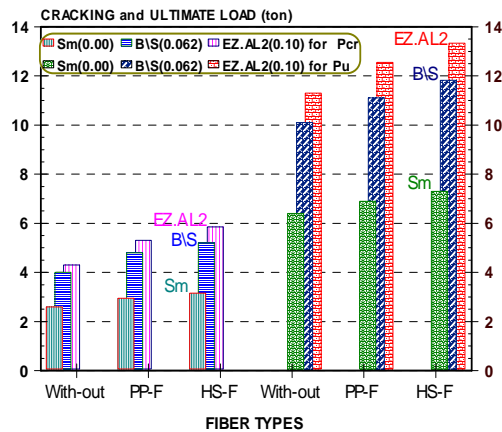


Fig 12: Cracking and ultimate loads of tested beams versus fibers type.

4. 2 Measured Deformations

The values of the obtained deformation at cracking (P_{cr}) and the ultimate loads (P_u) for tested beams are given in **Tables 6, 7, 8** and **9**. The values of this deformation depend on the grade of steel and its relative rib area (α_{sb}), and the fiber type.

4. 2. 1 Mid-span deflections

The values of deflection and the loads are considerably affected by the following parameters, as shown in **Table 6** and **Fig. 13**.

Table 6: Values of experimental deflection at cracking and ultimate loads and load at different values of deflection.

Group No.	Series	Fiber Types	Relative Rib Area (α_{sb})	Load (ton) at Deflection		Deflection, (mm) at P_{cr} (δ_{cr})	Deflection, (mm) at P_u (δ_u)
				0.5 mm	5 mm		
A	B1	Without Fiber	0.000	0.87	4.72	1.34	16.21
	B2		0.062	1.16	6.6	1.53	12.25
	B3		0.100	1.30	7.12	1.62	11.3
B	B1P	PP.F	0.000	1	5.07	1.27	15.25
	B2P		0.062	1.36	7.07	1.48	11.7
	B3P		0.100	1.57	8	1.53	10.9
C	B1S	HS.F	0.000	1.2	5.25	1.23	14.75
	B2S		0.062	1.56	7.56	1.45	10.8
	B3S		0.100	1.78	9	1.47	10.5

-Influence of grade of steel and its relative rib area (α_{sb})

At the same values of the deflections, the loads increase with the increase of grade of steel bar and its relative rib area (α_{sb}). The loads were increased by different percentages ranged from 30% to 57 % at deflection = 0.5 mm. But, this increase ranged from 33% to 71.4 % at deflection = 5 mm.

At the cracking loads, deflection increases with the increase of the relative rib (α_{sb}) due to increase of the cracking loads and constant stiffness of beams. The deflection was increased by different percentages ranging from 14.2 to 21 %.

At the ultimate loads, deflection decreases with the increase of the relative rib (α_{sb}). The deflection was decreased by different percentages ranged from 23.3 to 30.3 %. The reduction of the values of deflection for the beams reinforced with steel bar (EZ.AL2), (B\S) having ($\alpha_{sb} = 0.10, 0.062$) with higher values of yield stress may be due to the increase of the bond strength and the decrease of the slip resulting from the increase of the relative rib area (α_{sb}) and the decrease in number, length and width of cracks. Therefore, the stiffness of these beams were more than the corresponding stiffness for beams reinforced with steel bar (Sm) having ($\alpha_{sb} = 0.0$ & $F_y = 3100 \text{ kg/cm}^2$).

-Influence of fibers type

At the same values of deflection, the loads increase with the used fibers in reinforced concrete. The loads were increased by different percentages ranged from 15% to 37.9% for deflections = 0.5 mm. Whereas these increases ranging from 7.1% to 26.4 % for deflections = 5 mm.

At the cracking load, deflection decreases with the used fibers in reinforced concrete. The deflection value was decreased by different percentages ranged from 3.27 % to 9.3 %. At the ultimate loads, deflection decreases with the used fibers in reinforced concrete. The deflection value was decreased by different percentages ranged from

3.5 % to 11.84 % .The decrease of deflection with the used fibers in reinforced concrete resulting to decrease of slip and increase of bond strength, which accompanied with the decrease of length and width of cracks. Therefore, the stiffness of these beams with the used fibers in reinforced concrete were more than those for beams without fibers as shown in **Fig. 14**.

Table 7: Values of slip at cracking and ultimate loads and loads at different slips.

Group No.	Series	FIBER TYPES	Relative Rib Area(α_{sb})	Load, (ton) at Slip (mm)		Slip, (mm) at P_{cr}	Slip, (mm) at P_{ul}
				0.025	0.25		
A	B1	Without Fiber	0.000	0.08	0.75	0.81	2.25
	B2		0.062	0.17	2.05	0.47	1.34
	B3		0.100	0.24	2.65	0.40	1.19
B	B1P	PP.F	0.000	0.12	1.17	0.67	1.90
	B2P		0.062	0.36	3.86	0.32	1.09
	B3P		0.100	0.5	4.8	0.28	0.96
C	B1S	HS.F	0.000	0.16	1.5	0.58	1.75
	B2S		0.062	0.41	4.51	0.29	0.95
	B3S		0.100	0.63	5.85	0.25	0.84

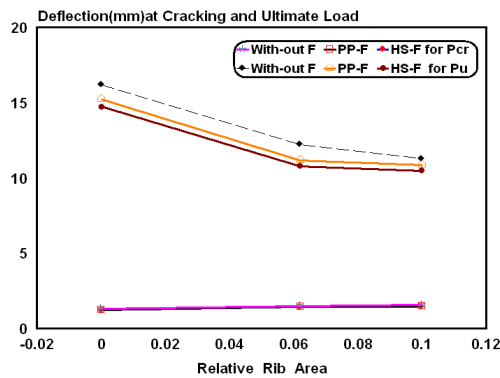


Fig. 13: Deflection at cracking and ultimate load versus relative rib area of tested beams.

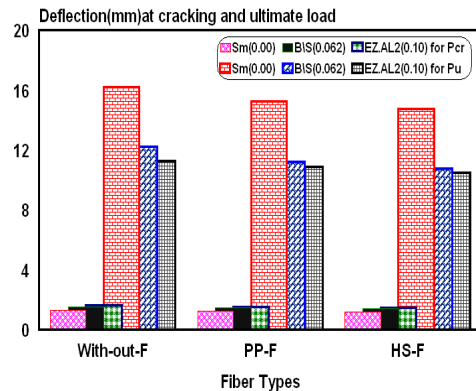


Fig. 14: Deflection at cracking and ultimate load versus fibers type of tested beams.

4. 2. 2 End slip of steel

The values of slip at cracking and ultimate loads and the loads are considerably affected by the following parameters: -

– Influence of grade of the main steel and its relative rib area (α_{sb})

The measured end slip of steel bars of tested beams as affected by grade of steel or its relative rib area are shown in **Table 7** and **Fig. 15**. At the same values of the slip, the loads increase with the increase of the relative rib area (α_{sb}) due to increase of the bond

strength (f_b). The loads were increased by different percentages ranged from 112.5% to 317% for slip = 0.025 mm and from 110 % to 285% for slip = 0.25 mm. At the same values of loads, the slip decreases with the increase of the grade of steel and its relative rib area (α_{sb}) due to increase of the bond strength (f_b).

At the cracking and the ultimate loads, the slip decreases with the increase of the relative rib area (α_{sb}) . The slip were decreased by different percentage ranged from 50.4% to 56.9 % for the cracking loads and from 47.1% to 52% for the ultimate loads. The decrease due to increase of the bond strength and the decrease in number, length and width of cracks. Therefore, the stiffness of the cross-section of beams was increased.

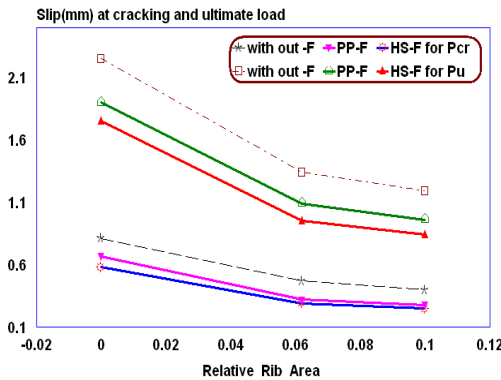


Fig. 15: Slip at cracking and ultimate load versus relative rib area of steel bar for tested beams.

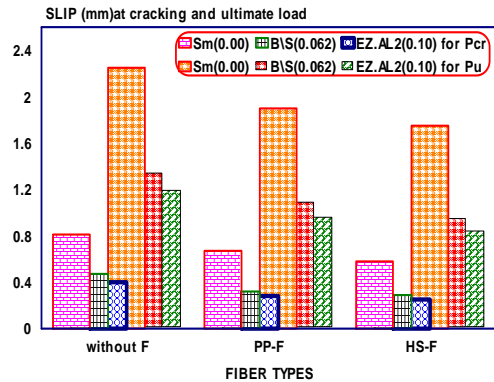


Fig. 16: Slip at Cracking and Ultimate Load versus fiber types for tested beams.

- Influence of fibers type

The measured end slip for steel bars of tested beams with and without fibers are shown in **Fig. 16** and **Table 7**. At the same values of slip, the loads increase with the used fibers in (HPC). They increased by different percentages ranged from 50% to 163% for slip = 0.025 mm and from 56 % to 102.7 % for slip = 0.25mm.

At cracking load, the slip decreases with the used fibers in (HPC) by different percentages ranged from 17.3 % to 38.3 %. At the ultimate load, the slip decreases with the used fibers in (HPC) by different percentages ranged from 15.56 % to 37.5 %. The measured end slip for tested beams group (C), of harex steel fibers, were less than that measured for group (B) of polypropylene fibers. Also, the measured end slip for tested beams group (B) having polypropylene fibers were less than that measured for tested beams group (A) without fibers.

4. 2. 3 Concrete strain

The values of concrete strain are measured at top surface of the compression zone corresponding to the relative rib area (α_{sb}), fiber types, cracking and ultimate loads and shown in **Table 8**. The values of concrete strain at cracking and ultimate loads and the loads are considerably affected by the following parameters:

Table 8 : Values of concrete strain at cracking and ultimate loads and loads at concrete strain = $0.07, 0.7 \cdot 10^{-3}$ m/m.

Group No.	Series	Fiber Types	Relative Rib Area(α_{sb})	Load (ton) at Strain $\cdot 10^{-3}$		Strain $\cdot 10^{-3}$ at P_{cr}	Strain $\cdot 10^{-3}$ at P_u
				0.07	0.70		
A	B1	Without fibers	0.000	1.0	6.2	0.18	0.75
	B2		0.062	1.75	7.28	0.24	1.29
	B3		0.100	2.0	7.59	0.25	1.46
B	B1P	PP.F	0.000	1.2	6.38	0.20	0.85
	B2P		0.062	2	7.53	0.25	1.45
	B3P		0.100	2.25	8	0.28	1.62
C	B1S	HS.F	0.000	1.5	6.6	0.21	0.93
	B2S		0.062	2.2	7.76	0.26	1.56
	B3S		0.100	2.4	8.41	0.30	1.69

- Influence of grade of main steel and its relative rib area (α_{sb})

Influence of grade of steel represented by its relative rib area on the concrete strain of all tested beams is shown in **Fig. 17** and **Table 8**. At the same values of strain, the loads increase with the increase of the relative rib area (α_{sb}) by different percentages ranged from 46.7 % to 100 % for strain = $0.07 \cdot 10^{-3}$ and from 17.4 % to 27.4 % for strain = $0.7 \cdot 10^{-3}$. This increase due to the decrease of slip, length and width of cracks.

At cracking load, the concrete strain increases with the increase of the relative rib area (α_{sb}) by different percentages ranged from 23.8% to 42.8 %. At the ultimate load, concrete strain increases with the increase of the relative rib area (α_{sb}) by different percentages ranged from 67.8 % to 94.7 %.

The increase of the values of concrete strain at cracking and ultimate loads for beams reinforced with steel bar having more relative rib area (α_{sb}) may be due to the bond strength increase and decrease of the slip between main steel and concrete for beams resulting from the decrease in length and width of cracks. Therefore, the stiffness of these beams were more than the beam with main steel of less relative rib area (α_{sb}).

- Influence of fibers type

Influence of fibers type on the concrete strain of all tested beams is shown in **Fig. 18** and **Table 8**. At the same values of strain, the loads increase with the used fibers in (HPC) by different percentages ranged from 20% to 50% at strain = $0.07 \cdot 10^{-3}$ and ranged from 3 % to 1.8 % at strain = $0.7 \cdot 10^{-3}$. At cracking load, the strain increases with the used fibers in (HPC) by different percentage range ranged from 4.16 % to 20 %. At ultimate load, the strain increases with the used fibers in (HPC) by different percentages ranged from 10.95 % to 24 % compared to those without fibers.

At cracking and ultimate loads, the values of concrete strain increase for beams with polypropylene and harex steel fibers than beams without fibers. Also the values of concrete strain increase for beams with harex steel fibers than beams with

polypropylene fibers. The increase of the values of concrete strain at cracking and ultimate loads for beams with polypropylene and haxex steel fiber may be due to the increase of bond strength and decrease of slip between main steel and concrete resulting from the decrease in length and width of cracks. Therefore, the stiffness of these beams became more than that of beams without fibers.

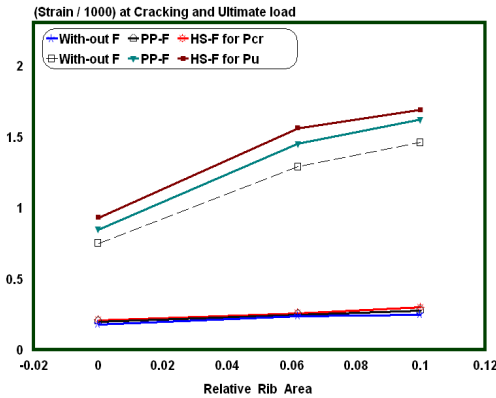


Fig. 17: Concrete strain at cracking and ultimate load versus relative rib area of tested beams.

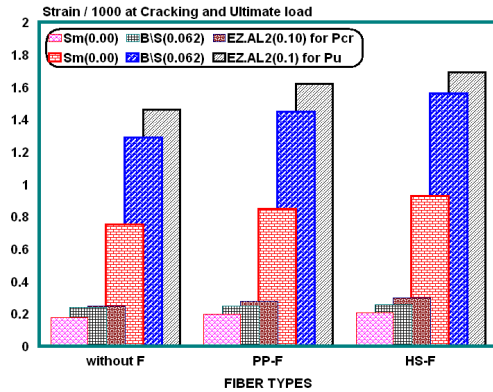


Fig. 18: Concrete strain at cracking and ultimate load versus fibers type for tested beams.

4. 2. 4 End slope of tested beams

The measured values of slope at the support of the beams corresponding to the point of maximum slope at cracking and ultimate loads are recorded in **Table 9**. The values of slope at the cracking and the ultimate loads and the loads at different slopes are considerably affected by the following parameters:

- Influence of grade of main steel and its relative rib area (α_{sb})

Influence of grade of steel represented by its relative rib area on the end slope of all tested beams is shown in **Fig. 19** and **Table 9**. At the same values of slope the values of loads increase with the increase of grade of steel and its relative rib area (α_{sb}). At the cracking loads, the slope of tested beams at the support increased with the increase of the relative rib area (α_{sb}) due to the increase of cracking loads and constant stiffness of the cross-section of the beam. At the ultimate loads, the slope of beams at the support decreased also with the increase of the relative rib area (α_{sb}) and grade of steel due to the decrease of slip and increase of bond strength, which causes a decrease in length, and width of cracks.

- Influence of fibers type

Influence of fibers type on the end slope of all tested beams is shown in **Fig. 20** and **Table 9**. At constant slope, the values of load carrying capacity of beams increase with the used fibers due to increase of bond strength and decrease of slip which causes decrease in length, width of cracks and increase stiffness of the cross-section of the beam.

At the cracking load, the slope values for beams increase with the used fibers due to increase of cracking load and constant value of stiffness of the beam. The reduction of the values of slope at ultimate loads for beams with harex fibers are due to the increase of bond strength and decrease of slip which causes decrease in length, width of cracks and increase the cross-section stiffness of the beams.

Table 9: Values of slope at cracking and ultimate loads and loads at different slopes.

Group No.	Series	Type of fiber	Relative Rib Area (α_{sb})	Load,(ton) at Slope, (radian)		Slope $\cdot 10^{-3}$ at cracking load (P_{cr})	Slope $\cdot 10^{-3}$ at ultimate load (P_{u0})
				0.001	0.01		
A	B1	Without Fiber	0.000	1.50	5.27	1.68	20.3
	B2		0.062	2.0	8.0	1.98	15.9
	B3		0.100	2.15	9.05	2.1	14.6
B	B1P	PP.F	0.000	1.55	5.67	1.60	19.75
	B2P		0.062	2.21	8.71	1.91	15.2
	B3P		0.100	2.56	10.38	1.98	14.14
C	B1S	HS.F	0.000	1.76	6	1.56	18.85
	B2S		0.062	2.47	9.46	1.88	13.99
	B3S		0.100	2.7	11.78	1.91	13.65

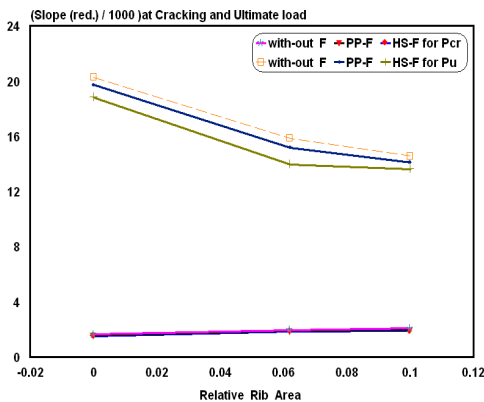


Fig. 19: Slope at cracking and ultimate load versus relative rib area for tested beams.

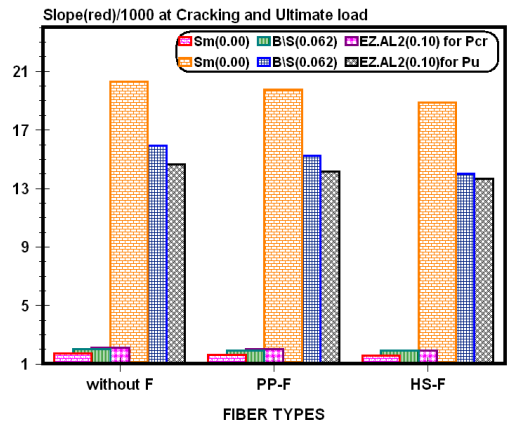


Fig. 20: Slope at cracking and ultimate load versus fiber types for tested beams.

CONCLUSIONS

1. The shape of rib geometry of steel bars represented by its relative rib area (α_{sb}) has a very small effect on their mechanical properties especially yield stress and ultimate strength and the main influence depends on the grade of steel.
2. The shape of rib geometry has a clear influence on the ultimate bond strength of tested specimens, which increased by about 139% by the increase of the relative rib area from 0.0 to 0.10 and not mainly depended on the yield stress of steel bars.

3. The first crack was early observed for (HPFRC) beams with main steel bars having smaller values of yield stress and relative rib area (α_{sb}) and also for beams without fibers.
4. The width of cracks and spacing between them were significantly large for beams having smooth bars, but narrow for other beams having ribbed bars. The propagation of cracks for beams reinforced with ribbed bars were more than those of beams reinforced with smooth bars.
5. The values of cracking and ultimate load carrying capacity of R.C. tested beams were increased with the increase of the yield stress and relative rib areas of main steel (α_{sb} from 0.0 to 0.10) by about 65 & 76% respectively for beams without fibers. Also, they were increased by about 80 & 82% for beams with polypropylene fibers and by about 86 & 83% for beams with harex steel fibers.
6. Adding fibers to the concrete mixes of (HPC) beams showed consistent higher first cracking and higher ultimate loads than those without fibers. Also adding harex steel fibers to the high strength R.C. beams showed consistent higher first cracking and ultimate loads than those of beams with polypropylene fiber.
7. The values of the deflection, strain, slip and end slope at free end of tested beams were decreased with the increase of the yield stress and relative rib area (α_{sb}) of the main steel.
8. Adding fibers to the concrete mixes of (HPC) beams showed smaller values of deflection, strain, slip and slope than those of beams without fibers. Also, they were less for beams with harex steel fibers than those of beams with polypropylene fibers.
9. The addition of fibers to concrete mixes of R.C. beams has greatly improved their ductility by increasing the ultimate strains under maximum compressive stresses and improved the crack propagation patterns for all tested (HPFRC) beams.
10. High strength fiber R.C. beams showed smaller crack widths and numbers compared to high strength R.C. beams without fibers at the same loading levels. Also, tested beams with harex steel fibers showed smaller crack widths and numbers compared to test beams with polypropylene fibers at the same loading levels.

REFERENCES

- [1] ACI 318R-95, "Building code Requirement for structure concrete and commentary", American concrete Institute, Detroit, Michigam, 1995.
- [2] Hosny M. Soghair, Mohamed M. Rashwan, Aly Abdel-Zaher Elsayed and Ali Mohamed Abdallah, " Effect of rib geometry of steel bars on bond strength for high performance concrete ", Journal of Engineering Sciences, Assiut University, Vol.33, No. 5, pp.1733-1748, September 2005.
- [3] Noumowe, " Mechanical properties and microstructure of high strength concrete containing polypropylene fibers exposed to temperature up to 200°C", Cement and Concrete Research, Vol. 35, Issue 11, November 2005, pp.2192-2198.
- [4] K. B. Lub and M. S. Mathews, " Influence of steel fibers on the behavior of conventionally reinforced thin-walled hollow beams' International Journal of Cement Composites and Light Concrete, Vol. 11, Issue 1, February 1989, p. 47.

- [5] P. N. Balaguru and S. P. Shah. (1992). Fiber Reinforced Cement Composites. McGraw-Hill, New York, 1992, xii, 530 pp.
- [6] C. Fritz, A. E. Naaman, and D.H.W. Reinhardt. (1992). Sifcon Matrix in RC Beams. Proceedings of the RILEM-ACI International Workshop, held June 23-26, 1991, Mainz, Germany; Ed. by H. W. Reinhardt and A. E. Naaman, E & FN Spoon, London, pp. 518-528.
- [7] M. H. Harajli and M. E. Mabsout (2002) M. H. Harajli and M. E. Mabsout (2002) "Evaluation of Bond Strength of Steel Reinforcing Bars in Plain and Fiber-Reinforced Concrete" ACI Structural Journal , July (2002)Vol. 99, No. 4.
- [8] Magdy A. Tayel et al (2003) "Experimental study on steel fiber-reinforced concrete beams "Tenth international colloquium on structural and geotechnical engineering April 22-24 , (2003) , Ain Shams University , Cairo , Egypt) .
- [9] Ali M. Abdallah "Effect of rib geometry for steel reinforcements on bond characteristics and rotational capacity of exterior joints in structures " M.sc.thesis. Assiut university ,(2000) .
- [10] Rehm , G, Eligehausen and Neubert , B.Erlauterung der Bewehrungsrichtlinien (Rationale for the detailing provisions of DIN 1045) Deutscher Ausschuss Fur Stahlbeton , Heft 300,1979.
- [11] Soretz, S., Holzenbein, H., " Einfluß der Rippenabmessungen von Betonbewehrungsstäben auf den Verbund und die Biegefähigkeit " Betonstahl in Entwicklung. Tor-Isteg Steel Corporation. Luxemburg , Heft 69, 1980.
- [12] Parviz Soroushian, Ki-Bong Choi, Gill-Hyun ,and Farhang Asiani " Bond of Deformed Bars to Concrete Effects of Confinement and Strength of Concrete .ACI Materials Journal V. 88 No.3 , May –June 1991 .
- [13] F. de Larrard, I. Schaller, and J. Fuchs. (1993). Effect of Bar Diameter on the Bond Strength of Passive Reinforcement in High-Performance Concrete. ACI Materials Journal, Jul-Aug, Vol. 90, No. 4, p. 333.

تأثير هندسية النتوعات وجودة حديد التسليح الرئيسي علي سلوك الانحناء للكمرات الخرسانية المسلحة عالية المقاومة و ذات الألياف تحت تأثير الأحمال الإستاتيكية

في الأونة الأخيرة ظهرت الحاجة الماسة لاستخدام الخرسانة ذات المقاومة العالية وذلك لاستخدامها في المباني ذات الارتفاعات العالية وكذلك في الخرسانات الثقيلة في المنشآت البحرية. من المعروف أن استخدام خرسانة عالية المقاومة يتطلب نسبة عالية من حديد التسليح (تصل إلى حوالي 7% من مساحة القطاع) للحصول علي أقصى مقاومة في الانحناء لأي عنصر إنشائي. لذلك أصبح من الضروري استخدام حديد تسليح عالي الجودة للاستفادة من أقصى مقاومة له مع الخرسانة ذات المقاومة العالية. لذا فان الأمر يتطلب قوة تماسك كافية بين الحديد و الخرسانة مما يستلزم أن يحاط سطح حديد التسليح بنتوعات تكفل تولد قوى التماسك الكافية بينهما. ونظرا لاختلاف هندسية النتوعات لأنواع حديد التسليح وجودته المختلفة فقد ظهرت الحاجة لمعرفة اثر هذا الاختلاف علي سلوك العناصر الإنشائية من الخرسانة عالية المقاومة.

وحيث أن الخرسانة ذات المقاومة العالية مادة قصفة وقليلة الممتطولية لذا احتاجت الخلطة الخرسانية إلى بعض الإضافات مثل الألياف لتحويلها إلى مادة ذات ممتطولية . ونظرا لقلة المعلومات المتوفرة عن سلوك الانحناء للكمرات الخرسانية المسلحة المصنعة من الخرسانة عالية المقاومة بدون الألياف و ذات الألياف مع الأخذ في الاعتبار بعض المتغيرات التي تؤثر على هذا السلوك مثل المساحة النسبية للنتوء لحديد التسليح الرئيسي وجودته . لذلك فان هذا البحث يركز علي تطبيق واستخدام أنواع مختلفة من الألياف وحديد تسليح ذي جودة وبتنوعات مختلفة في تكنولوجيا إنتاج كمرات خرسانية مسلحة عالية المقاومة ثم دراسة تأثير هندسية النتوءات لحديد التسليح الرئيسي وجودته وكذلك نوع الألياف علي سلوك الانحناء لها تحت تأثير الأحمال الاستاتيكية .

وقد تم ذلك بإجراء اختبارات معملية علي عدد 9 كمرات خرسانية مسلحة ذات مقاومة عالية (900 كجم / سم²) وقد تم تقسيمها إلى ثلاث مجموعات . المجموعة الأولى تتكون من عدد 3 كمرات بدون ألياف ، والمجموعة الثانية تتكون من 3 كمرات بها ألياف البولي بروبيلين بنسبة 1% بالحجم من الخلطة ، أما المجموعة الثالثة فتتكون من 3 كمرات بها ألياف حديد الهاركس بنسبة 1% بالحجم من الخلطة. وهذه الكمرات الخرسانية ذات قطاع ثابت 12×30سم وتسليح سفلي رئيسي = 2Ø16مم وعلوي 2Ø12مم وكانات = 10 Ø 8 مم/متر. طول البحر الفعال للكمرات المختبرة = 240 سم ، أما البحر الكلي للكمرات = 240 سم + 5 مرات قطر السيخ من كل جانب. وقد تم الأخذ في الاعتبار المتغيرات التالية :

- هندسية النتوءات ومعبر عنها بالمساحة النسبية للنتوء لحديد التسليح الرئيسي المستخدم في عينات الاختبار وقيمها هي (0.0 ، 0.062 ، 0.10) وكذلك جودة حديد التسليح ومعبر عنها بمقاومة الخضوع وقيمها (3100 للحديد الأملس، 4600، 4750 كجم/سم² للحديد المشرشر) .
- نوع الألياف المستخدمة (ألياف البولي بروبيلين وألياف الهاركس بنسبة 1% بالحجم من الخلطة الخرسانية) - وقد تم استخدام رتبة واحدة من الخرسانة عالية المقاومة وكانت قيمتها هي (900 كجم/سم²) ، وكذلك نسبة واحدة من تركيز الألياف للخلطة وذلك لمقارنة النتائج.

وقد تم التوصل لنتائج هامة في هذا البحث منها ما يلي :

- طراز الانهيار وسلوك الانحناء للكمرات الخرسانية المسلحة عالية المقاومة بدون الألياف وذات الألياف يعتمد علي هندسية النتوءات لأسياخ حديد التسليح الرئيسي وجودته وكذلك علي نوع الألياف المستخدمة .
- استخدام الألياف في الكمرات الخرسانية يؤدي إلى تقليل الشروخ و زيادة المسافة بينها وزيادة أحمال التشريح وأقصى حمل وزيادة الممتطولية للكمرات الخرسانية و نقص التشكلات الحادثة كالترخيم وانزلاق الحديد مع الخرسانة .
- هندسية النتوءات لأسياخ حديد التسليح الرئيسي لا تؤثر علي خواصه الميكانيكية ولكن تؤثر بشكل واضح علي أقصى اجهادات تماسك بين الحديد والخرسانة والذي يزيد بدوره بحوالي 139% بزيادة المساحة النسبية للنتوء إلي 0.10 بالمقارنة بعينات الحديد الأملس.